Advances in Concrete Construction, *Vol. 8, No. 2* (*2019*) *145-154*
DOI: https://doi.org/10.12989/acc.2019.8.2.145

Experimental study on effect of EBRIG shear strengthening method on the behavior of RC beams

Amir Shomali*[1], Davood Mostofinejad[1a] and Mohammad Reza Esfahani[2a]

[1]*Department of Civil Engineering, Isfahan University of Technology (IUT), Isfahan, Iran*
[2]*Department of Civil Engineering, Ferdowsi University of Mashhad, Mashhad, Iran*

(*Received May 9, 2018, Revised April 14, 2019, Accepted June 12, 2019*)

Abstract. The present experimental study addresses the structural response of reinforced concrete (RC) beams strengthened in shear. Thirteen RC beams were divided into four different sets to investigate the effect of transverse and longitudinal steel reinforcement ratios, concrete compressive strength change and orientation for installing carbon fiber-reinforced polymer (CFRP) laminates. Then, we employed a shear strengthening solution through externally bonded reinforcement in grooves (EBRIG) and externally bonded reinforcement (EBR) techniques. In this regard, rectangular beams of 200×300×2000 mm dimensions were subjected to the 4-point static loading condition and their load-displacement curves, load-carrying capacity and ductility changes were compared. The results revealed that using EBRIG method, the gain percentage augmented with the increase in the longitudinal reinforcement ratio. Also, in the RC beams with stirrups, the gain in shear strength decreased as transverse reinforcement ratio increased. The results also revealed that the shear resistance obtained by the experimental tests were in acceptable agreement with the design equations. Besides, the results of this research indicated that using the EBRIG system through vertical grooves in RC beams with and without stirrups caused the energy absorption to increase about 85% and 97%, respectively, relative to the control.

Keywords: CFRP; shear strengthening; externally bonded reinforcement in grooves (EBRIG); externally bonded reinforcement (EBR); ductility

1. Introduction

Over the recent decade, many investigations have been conducted on the shear strengthening of reinforced concrete (RC) beams by means of unidirectional or multi directional fiber reinforced polymer (FRP) materials to examine variables affecting the structural response of the beam (Mofidi and Challal 2014, Teng *et al*. 2002). The reason for the ever-growing utilization of composite materials is their remarkable features such as excellent strength-to-weight ratio, facile installation and noticeable corrosion resistance (Teng *et al.* 2002). Shear strengthening of RC members is viable through bonding the FRP sheets or strips around the section in different layouts. Strips or sheets of FRP laminates in full wrapping, U-wrapping and two sides could be designed and adhered to the beam faces with eligible directions to the beam's longitudinal axis (Chen and Teng 2003). Satisfactory laboratory and analytical verifications have made the conventional EBR method a welcomed solution to the shear and flexural strengthening goals over the past years. This approach is initiated by removing a few millimeters of an unreliable surface layer of concrete and then CFRP fabrics are connected to the member's substrate. Major factors that affect strengthening methods are the material properties (FRP and concrete), bond strength at the interface of FRP to concrete and the wrapping layout (Belarbi and Acun 2013).

Rita *et al*. (2003) bonded CFRP strips onto the side surfaces of large-scale RC beams to enhance their shear performance and convert their brittle shear failure to a ductile flexural manner. In their study, de-bonding of FRP strips caused by shear stresses of the cohesive layer remained as an important issue. To preclude this drawback, alternative strengthening methods may be utilized such as Near Surface Mounted (NSM) method and anchorage systems, which use metallic anchor bolts or FRP spikes but, entail heavy costs (De Lorenzis and Teng 2007, Galal and Mofidi 2010, Zhou *et al*. 2017). Recently, the grooving method (GM) has been proposed for shear, flexural and axial strengthening in RC members to eliminate de-bonding probability as the most dangerous failure mode for FRP strengthened members (Mostofinejad and Mahmoudabadi 2010, Mostofinejad and Moshiri 2014, Saljoughian and Mostofinejad 2018). GM can be performed in two ways: Externally bonded reinforcement on grooves (EBROG) and externally bonded reinforcement in Grooves (EBRIG). In both techniques, longitudinal or vertical shallow slits are created, respectively, on the tension face or lateral surface of RC beams and filled with epoxy resin. Therefore, in the EBROG method, composite strips are bonded onto the slits; but in the EBRIG technique, the strips are folded and bonded onto the surfaces of the slits and the adjacent areas of the slits at the level of the concrete surface.

The NSM shear strengthening procedure involves

*Corresponding author, Ph.D. Student
E-mail: Amir6002002@yahoo.com
[a]Professor

http://www.techno-press.org/?journal=acc&subpage=7
ISSN: 2287-5301 (Print), 2287-531X (Online)

creating hand-made grooves in the side faces of the concrete elements, and inserting FRP strips or bars in these grooves which are already filled with a suitable epoxy or mortar (De Lorenzis and Teng 2007, Mostofinejad *et al*. 2019). De Lorenzis and Rizzo (2009) conducted an experimental study using the NSM and the EBR techniques for shear rehabilitation of RC beams and resulted that these techniques increased the ultimate load by about 16% and 24%, respectively. The authors further reported delamination of the CFRP composites in both methods as engineering challenges.

In another attempt, Kuntal *et al*. (2017) manufactured 12 pre-stressed concrete beams with a shear span to depth ratio of 2.5 and subjected them to a bending test. All the specimens, with or without steel stirrups, were strengthened using various NSM CFRP installation schemes. The results of this work confirmed that CFRP laminates at 45°, compared with 90°, were more efficient in upgrading the shear strength and stiffness capacity as well as ductility in the beams with and without stirrups. They also pointed out that, the preferable ductile flexural failure was replaced by the brittle shear one, because of better restriction of crack propagation.

Mofidi *et al*. (2016) presented the results of a research comprised of six tests on RC T-beams shear strengthened using near-surface mounted FRP rods and internal stirrup. It was concluded that an appropriate strengthening configuration induces the formation of a distributed crack pattern and lead to the yielding of steel stirrups.

Mostofinejad and Tabatabaei Kashani (2013) introduced EBROG method for shear strengthening of RC members in technical literatures (Mostofinejad and Torabian 2015). They subjected 32 small-scale rectangular beams to the 4-point loading in order to substitute the grooving method with the EBR strengthening approach. These researchers concluded that by applying this procedure through cutting narrow slits into the beam's concrete cover, the catastrophic shear failure mode may be replaced by a flexure one and the ultimate load, withstood higher values, relative to the EBR strengthened beams.

Subsequent investigations of Mostofinejad *et al*. (2016) resulted in a novel solution for shear strengthening which is, herein, referred to as EBRIG method. In this approach, as the CFRP strips are glued to the groove surfaces through direct contact, the possibility for CFRP separation from the surface of the concrete is considerably reduced and stresses are better transmitted between the concrete and the composite materials (Shomali *et al*. 2019). The authors further observed that, with regard to the reference specimen, the values obtained for the energy absorption rate, were enhanced up to 320%.

The EBRIG method was further utilized for the purpose of flexural strengthening in RC beams by Mostofinejad and Shameli (2013). To prove the superiority of the EBRIG and EBROG methods over the EBR and NSM flexural strengthening methods, these researchers carried out tests on beams with small dimensions with CFRP laminates attached on the tension face. They showed that, the strengthened beams failed with no sign of premature de-bonding and their failure were due to the rupture of CFRP sheets.

Fig. 1 Steel reinforcing cage

In the present paper, in order to fully investigate the behavior of EBRIG shear strengthened RC beam, the effects of the concrete strength, the orientation of CFRP installing, and the changes in shear and flexural bar ratios, on the load carrying capacity, the mid-span displacement and the energy absorption rate, were investigated. Furthermore, an analytical study was carried out in accordance with the ACI provisions to express the ultimate shear resistance of the experimental tests. Also, the maximum strain values of the CFRP laminates over the main diagonal crack were measured by demountable mechanical strain gauge (DEMEC) to investigate the performance of strips.

2. Experimental procedure

The experimental program of this research includes 13 RC rectangular beams with a dimension of 2000×300×200 mm, classified into four series. The required dimensions and steel reinforcement bars of the strengthened and un-strengthened specimens were computed in advance to ensure the occurrence of a shear failure. To avoid the collapse of a deep beam (arching effect) based on the ACI 318-14 code, a shear span of 600 mm was considered in each sample (ACI Committee 318 2014). Fig. 1 shows the steel reinforcing cage in the mold for one of the specimens. A local supplier delivered the ready mix concrete to the structural laboratory. The target cylindrical concrete strength were considered 30 MPa (Normal strength concrete) and 55 MPa (High strength concrete). The mean value of concrete strength was measured by the compression test after 28 days of curing (ASTM C 39/C 2005). CFRP strips were made up of unidirectional carbon fibers and the wet layup procedure was applied for fabrics in both the EBR and EBRIG systems. For the EBRIG strengthening, a set of two parallel grooves (vertical or diagonal) were cut via grinding machine on two lateral sides of the beams, with 8 mm depth and 3 mm width. CFRP strips with 70 mm width and 300 mm length were then attached to the surfaces of the grooves alongside the beams; the strengthening strips were pressed by hands on the grooves, which were partially filled with epoxy (Fig. 2). Afterwards, the CFRP strengthening system was cured for a week to let the adhesive become sticky (Mesbah and Benzaid 2017). Table 1 presents the mechanical properties

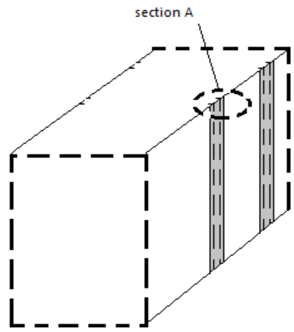

(a)

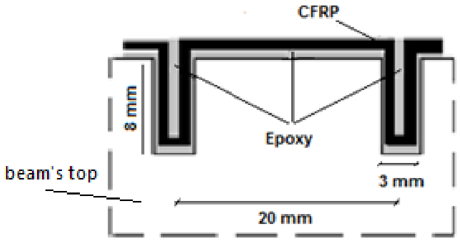

(b)

Fig. 2 Details of the proposed strengthening technique: (a) Schematic of the EBRIG strengthening method on the lateral side; (b) section A

of the epoxy and carbon fibers.

To test the efficiency of the EBRIG and EBR techniques, both strengthened and un-strengthened specimens were simply supported at two ends and examined under a monotonic four-point bending test with a loading rate of 2 mm/min. A digital data acquisition device linked to a computer system collected the signals coming from the

Table 1 Characteristics of the CFRP materials

Type		Thickness per layer (mm)	Tensile strength (MPa)	Tensile E-modulus (MPa)	Nominal elongation at break (%)
Dry Fiber	Quantom Wrap 200C	0.11	4042	228000	1.5
Adhesive	Quantom EPR 3301	0.5	42.1	4485	-

sensors (Fig. 3). Load-displacement curves were plotted using a linear variable differential transducer (LVDT) and a load cell transducer. Also, the maximum strain in fiber direction for the third CFRP strip from the support (approximate location of the major diagonal cracks in the shear zones) in each of the strengthened specimens was measured before the rupture of CFRP using a Demec gauge (Fig. 4). Demec gauges were applied successfully by Hosen *et al*. (2015) for reading sectional strain along the depth of specimens for NSM strengthened beams. It should be mentioned that failure may occur by simultaneous rupture of the second and third or the third and fourth CFRP strips with regard to the shear crack path; this shows that the maximum strains in the ruptured strips are relatively equal. The onset and propagation of cracks were specified on the lateral sides of the specimens and photographed during the testing. The test setup and its configuration are displayed in Fig. 3.

2.1 Description of specimens

The test beams included 13 specimens, (Table 2), categorized into the following 4 groups.

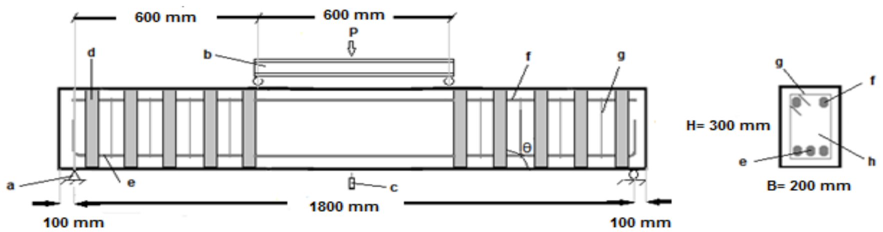

a- supports; b- load transferring system; c- LVDT; d- CFRP sheet; e- tensile reinforcing bars with 90-degree hooks; f- compressive reinforcing bars; g- steel stirrup; h- cross section of the beam.

(a)

(b)

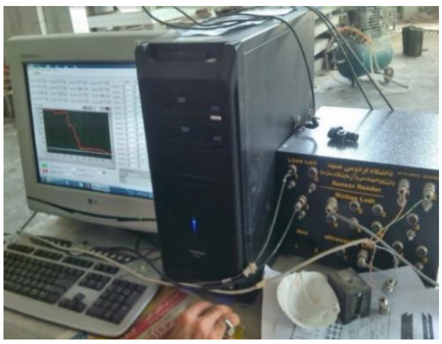

(c)

Fig. 3 Schematic view of the specimens and test setup: (a) details of the specimens (b) loading frame and test specimen; (c) data acquisition system

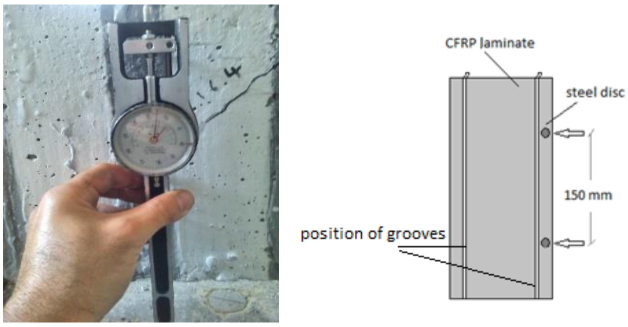

(a) (b)

Fig. 4 CFRP strain measuring: (a) Demec gauge on CFRP laminate; (b) position of steel discs for strain gauge reading

Table 2 Specifications of the specimens

Group	f'_c (MPa)	Label	Longitudinal reinforcement		Stirrup	θ (degrees)[a]
			Bottom	Top		
1	34	B1-EBRIG-V[b]-30[c]	3D16	2D12	-	90
	34	B2-EBRIG-V-30	3D20	2D12	-	90
	34	B3-Control-30	3D16	2D12	-	-
	34	B4-Control-30	3D20	2D12	-	-
	34	B5-EBR-V-30	3D20	2D12	-	90
2	32	B6-EBRIG-V-30	3D20	2D12	6-130 mm	90
	32	B7-EBRIG-V-30	3D20	2D12	6-198 mm	90
	32	B8-Control-30	3D20	2D12	6-130 mm	-
	32	B9-Control-30	3D20	2D12	6-198 mm	-
3	58	B10-EBRIG-V-55	3D20	2D12	6-198 mm	90
	58	B11-Control-55	3D20	2D12	6-198 mm	-
4	31	B12-EBRIG-D[d]-30	3D20	2D12	6-198 mm	45
	31	B13-EBRIG-D-30	3D20	2D12	-	45

[a]Angle of CFRP strips.
[b]Vertical CFRP laminates, inclination angle over longitudinal axis of beam equal 90°.
[c]Concrete compressive strength equal 30 or 55 MPa.
[d]Diagonal CFRP laminates, inclination angle over the axis of beam equal 45°.

2.1.1 Group 1

The five beams of this group were basically designed to investigate the changes in the amount of main bending bars, and their effects on the shear force gain through the EBRIG strengthening method. Two of the specimens operated as the control beams, two were strengthened at 90° with one layer of CFRP strips using EBRIG method and the last one was strengthened at 90° with one layer of CFRP strips using EBR technique. Two Control beams were reinforced with three 16 mm diameter bars and three 20 mm diameter bars at the bottom, respectively. Similar to the control beams, the two EBRIG strengthened beams, were reinforced with three 16 mm diameter bars and three 20 mm diameter bars at the bottom, respectively. The EBR strengthened specimen was reinforced with three 20 mm diameter bars at the bottom. In the specimens of all the test series, two 12 mm diameter bars were arranged in one layer at the top. Flexural bars in all the series had a yield stress of about 400 MPa. Given that exploiting FRP materials for shear strengthening is more efficient and practical in RC beams with no transverse steel (Grande *et al*. 2009), stirrups were not included in the specimens of this group. Another reason for using no stirrups in the specimens of this group is to decouple the effects of longitudinal bars and stirrups.

The prepared CFRP strips were 70 mm wide and spaced at 130 mm center-to-center for both the EBR and EBRIG strengthened specimens (five strips in each of the shear spans). The average concrete strength was 30 MPa in this group. To have an efficient reinforcing layout, a spacing less than d/4 was assumed between the CFRP strips in all the strengthened beams, according to the ACI 440.2R-08 provisions (ACI Committee 440 2008).

2.1.2 Group 2

This group consisted of four beams which was designed to realize the interaction between the internal shear reinforcements and the proposed strengthening system as an external shear strengthening technique. The specimens consisted of two control beams with 6 mm diameter bars as internally closed stirrups (yield stress of about 220 MPa), spaced at $s=d/2$ and $s=3d/4$, respectively. The other two specimens of this group were strengthened vertically using the EBRIG technique and were reinforced with 6 mm diameter bars as stirrups, spaced at $s=d/2$ and $s=3d/4$, respectively. In all specimens of this group, three 20 mm diameter bars at the bottom of the cross section and two 12

Table 3 Summary of the test results

Group	Label	Ultimate load (kN)	Mid-span displacement (mm) at ultimate load	Energy absorption (J)	Failure mechanism
1	B1-EBRIG-V-30	187	6.9	955	CFRP rupture and de-bonding
	B2-EBRIG-V-3	225	6.3	1175	CFRP rupture and de-bonding
	B3-Control-30	111	4.9	419	Shear Failure
	B4-Control-30	129	5.2	595	Shear Failure
	B5-EBR-V-30	172	5.6	755	CFRP de-bonding
2	B6-EBRIG-V-30	288	9.7	2150	CFRP rupture and de-bonding
	B7-EBRIG-V-30	269	7.7	1820	CFRP rupture and de-bonding
	B8-Control-30	220	8.5	1257	Shear Failure
	B9-Control-30	181	6.1	988	Shear Failure
3	B10-EBRIG-V-55	336	9.8	2300	CFRP rupture and de-bonding
	B11-Control-55	282	8.6	1750	Shear Failure
4	B12-EBRIG-D-30	293	8.2	1975	CFRP rupture
	B13-EBRIG-D-30	251	7.3	1400	CFRP rupture

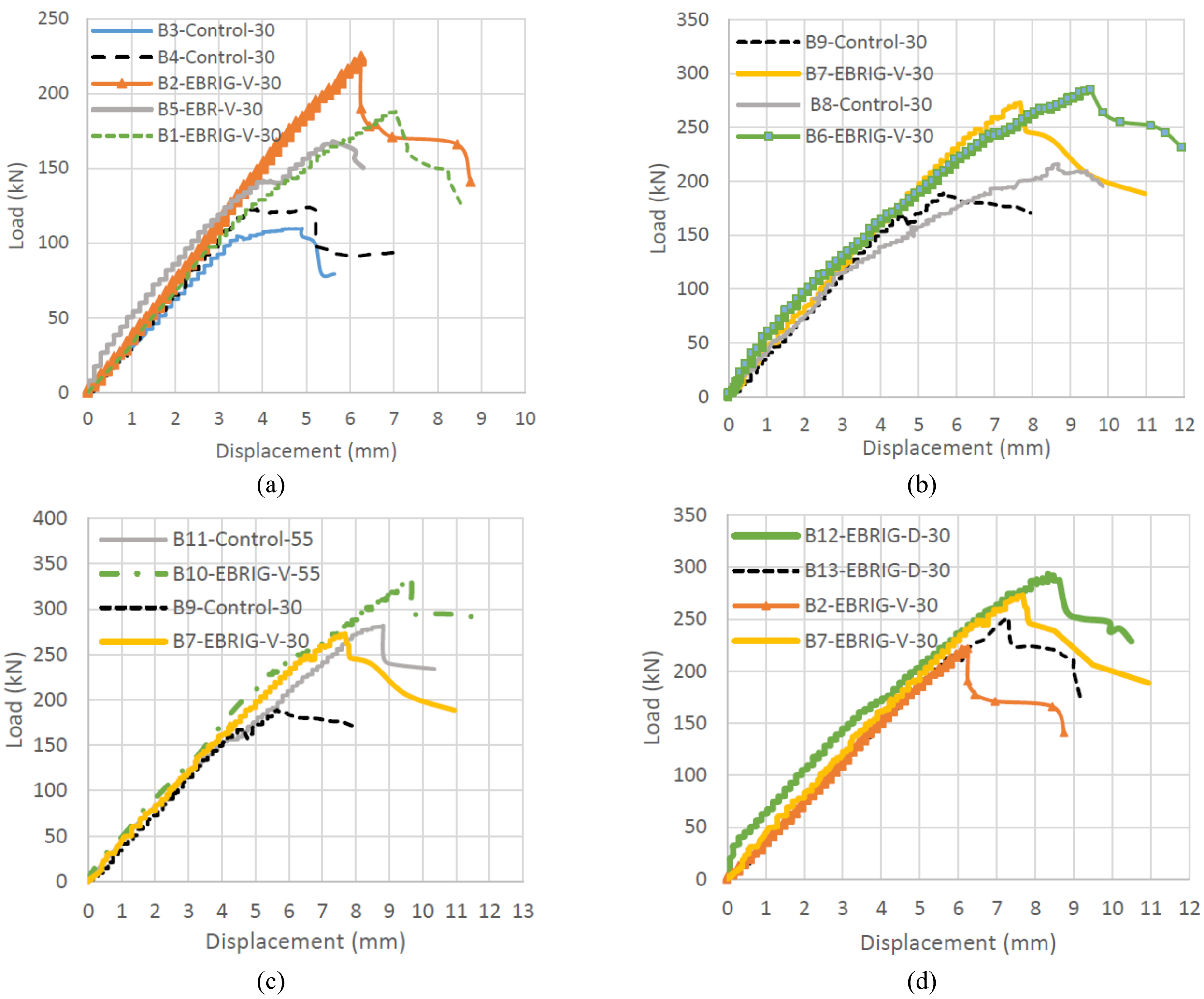

Fig. 5 Load-displacement diagrams for beams: (a) Group 1; (b) Group 2; (c) Group 3 and (d) Group 4

mm bars at the top acted as flexural reinforcements. The concrete compressive strength and other characteristics of the strengthening layout in this group were similar to those in Group 1.

2.1.3 Group 3

In this group, a 55 MPa compressive strength was considered for concrete in order that it falls in the range of high strength concretes to study its influence on the shear behavior of EBRIG strengthened beams. One of the specimens operated as the control beam, while the other were strengthened vertically with one layer of CFRP laminates using the EBRIG technique.

The flexural steel bars of the specimens were similar to that of Group 2. For transverse reinforcements, 6 mm diameter steel bars spaced at $s=3d/4$, were used.

2.1.4 Group 4

Two beams of this group were strengthened using one layer of CFRP laminates at 45° with regard to the longitudinal axis of the beam. The longitudinal steel bars of the specimens were similar to that of Group 2. Regarding transverse steel, however, one was strengthened with 6 mm diameter bars spaced at $s=3d/4$ and the other had no stirrups. The concrete compressive strength of specimens was considered to be 30 MPa.

3. Experimental results and discussions

3.1 Load-displacement curves and failure mechanism

Table 3 illustrates the maximum load carrying capacity values, the mid-span deflections and the ultimate failures of the specimens in each of the predefined groups. Furthermore, Fig. 4 demonstrates the load-displacement curves of the strengthened specimens and control beams in each group. As shown in Fig. 5, all the specimens have similar stiffness prior to the flexural cracks.

By an increase in the load, the stiffness of the EBRIG strengthened beams underwent no significant change, revealing that this feature is not highly sensitive to the novel technique. As seen in Fig. 5(a), the EBRIG strengthened beams exhibit a slightly lower stiffness compared with those strengthened via the EBR method. This result might be due to the difference in the stiffness between the two lateral covers of the beam and the concrete core, which probably induced internal cracks and reduced the stiffness

Fig. 6 Failure mode of specimen B4-Control-30

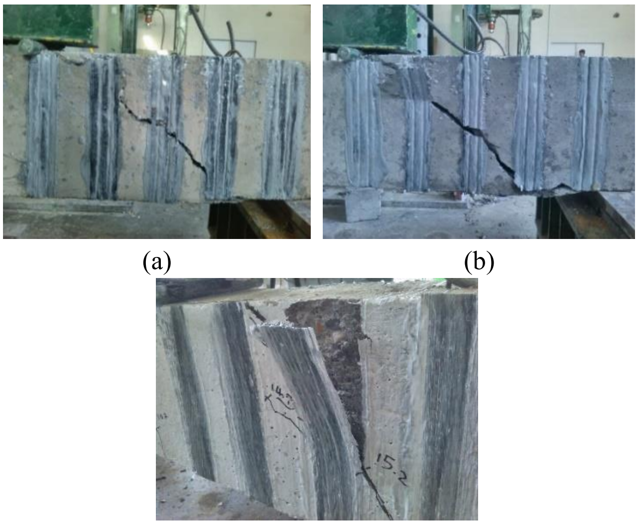

(a) (b)

(c)

Fig. 7 Failure modes of strengthened specimens in Group 1: (a) B1-EBRIG-V-30; (b) B2-EBRIG-V-30 and (c) B5-EBR-V-30

of the EBRIG strengthened beams at the initial stages of loading.

As far as control beams are concerned, the shear failure mode occurred abruptly with diagonal cracks, spreading out from the loading points toward the supports at both ends, at the final stages of loading (Abdel-Kareem 2014). Fig. 6 displays specimen B4 after the beam failure.

In Group 1, the failure of the EBR strengthened beam occurred with greater load and mid-span deflection, compared to its corresponding control beam; Specimen B2 (EBRIG method), on the other hand, carried more load capacity and failure deflection relative to the EBR strengthened one. Owing to the complete bond between composite strips and the concrete substrate in B2, an approximate increase of 30% and 12% were observed in the maximum load and mid-span deflection, respectively, relative to EBR. Additionally, specimens B1 and B2 showed 68% and 74% increases in the ultimate load, relative to their corresponding reference beams. Therefore, increasing longitudinal steel reinforcement ratio in the EBRIG strengthened beams, led to increase in the shear capacity of the beams. Fig. 5(a), shows that the higher reinforcement ratio in specimen B2 improved the overall stiffness and ultimate load compared with specimen B1. The control and EBR strengthened beams underwent a noticeable change in the slope of their load-deflection curves which might be due to the yielding of flexural reinforcements. Fig. 7 shows the

(a) (b)

Fig. 8 Failure modes of strengthened specimens in Group 2: (a) B6-EBRIG-V-30; (b) B7-EBRIG-V-30

development of critical shear crack and the failure modes of the strengthened beams in Group 1. In the EBR strengthened specimens, due to the high interfacial shear stress around the main shear crack, the middle CFRP strip deboned and caused a premature failure in the beam. As shown in Fig. 7, in the specimens strengthened via the EBRIG method, by increasing the stresses in the middle of the shear span, the main shear crack becomes wider, inducing CFRP rupture; partial de-bonding from lateral faces of the beams was also observed in the strengthened specimens. The analysis of test data (Table 3) pertaining to Group 2 demonstrates, that B6 and B7 failed when the maximum applied loads reached 288 and 269 kN, respectively, suggesting, that shear capacity increased 30% and 48% relative to their corresponding un-strengthened beams, respectively. The experimental results showed that with an increase in the amount of transverse steel reinforcement, the percentage of gain in the ultimate load decreased, probably owing to the interaction between CFRP strips and steel stirrups. Comparing the maximum measured deflection values of B6 and B7 with their corresponding un-strengthened beams, revealed, that the increase in the internal transverse steel reinforcement reduced deformability by 12%. Fig. 5(b) shows the load versus displacement curves. As can be seen, following the crack, the overall stiffness of specimen B6 is slightly higher than B7, probably due to its more internal transverse reinforcement. These beams had similar stiffness values and structural performance at the early stages of loading, implying that prior to the flexural cracks, the load was carried predominantly by the concrete itself. The shear performance of the beams strengthened with CFRP strips in this group is similar to that of Group 1; with their failure presented in Fig. 8.

Table 3 demonstrates the effect of increase in the concrete strength, which postponed the ultimate failure, thereby improving the load carrying capacity. In this group, the enhancement in the ultimate load and the mid-span deflection of B10, compared with its corresponding reference beam, were 19% and 13%, respectively. However, the ultimate load and deflection for specimen B7, increased by 48% and 26%, relative to the control beam in

Group 2 and shows more effectiveness of normal strength concrete in improving the behavior of beams. Al-Tersawy (2013), also established the fact that shear strengthening through FRP sheets was more effective in RC members made of normal strength concrete. Fig. 9 shows the failure modes of strengthened and un-strengthened

(a) (b)

Fig. 9 Failure modes of specimens in Group 3: (a) B11-Control-55; (b) B10-EBRIG-V-55

(a) (b)

Fig. 10 Failure modes of strengthened specimens in Group 4: (a) B12-EBRIG-D-30; (b) B13-EBRIG-D-30

beams in Group 3. The failure occurred due to the rupture of CFRP over the main shear crack and de-bonding of its neighboring strips. The overall stiffness of B10 was slightly more than B7 and B9. Both specimens in this group exhibited a sudden drop after reaching peak point in the load-displacement curve due to the brittle nature of high strength concrete (Fig. 5(c)). The brittleness of a member affects both post-cracking and fracture behavior of concrete (Satish Kumar *et al*. 2017). As can be seen from Table 3, the inclined CFRP laminates employed in the EBRIG system in Group 4, are more capable of upgrading shear capacity comparisons with the vertical ones. The main reason for this result is the inhibiting mechanism that acts perpendicular to the inclined shear crack and the higher bond length of inclined CFRP materials.

Abdul Samad *et al*. (2017) also reached this finding in the shear strengthening of RC beams via EBR. It should be noted that the inclined EBRIG system can better carry tensile loads when the shear cracks appear in an orthogonal direction. Moreover, it is ill-advised to employ a 45° installation of the composite in RC beams for seismic designing. The application of CFRP strips at 45° direction resulted in a 9% enhancement in the ultimate load carrying capacity of the beam with stirrups, relative to the beams strengthened with vertical CFRP strips in Group 2; the ultimate load carrying capacity of B13 increased by 11%, relative to B2, implying that the inclined utilization of CFRP strips is more effective when transverse steel reinforcements exist. Fig. 5(d) shows the load-deflection diagrams pertaining to certain EBRIG strengthened beams in Groups 1, 2 and 4, wherein a relatively similar behavior prior to and following peak load can be observed. As shown in Fig. 10, the most stressed CFRP strip was ruptured without any sign of de-bonding in other strips.

3.2 Ductility of the specimens

Researchers have endeavored to improve the ductility of a concrete element especially in the seismic zones, as it causes beams to experience plastic deformations; hence, warning signs prior to the catastrophic failure are observed due to stress distribution (Gunes *et al*. 2013). To compare this parameter among the strengthened RC beams, the area under the load-deflection diagram up to the ultimate failure was computed as the energy absorption, a suitable criterion for the ductility differences (Sumathi and Arun Vignesh 2017); these values are presented in Table 3 for specimens of all the series. As presented in Table 3, specimens B3 and B4 (control beams) in Group 1, absorb 425 and 590 J (kN.mm) energies due to the concrete cracking and flexural reinforcements. The area under the load-deflection curves in specimens B1 and B2, specified an energy absorption of 955 and 1175 J, suggesting 127% and 97% increases in ductility, relative to the control beams, respectively. This also shows that the lower the ratio of flexural reinforcements, the higher the energy absorption rate will be. In this group, by increasing the energy absorption, the EBR strengthened beam exhibited a 26% improvement in ductility. It can be concluded from the results that the EBRIG technique significantly increases the ductility of un-strengthened beams.

Specimens B6 and B7 in Group 2 exhibited 2150 and 1820 J, respectively as the absorption energy values. In other words, the values in these specimens enhanced by 71% and 84%, relative to their corresponding control beams. This result proves that increasing internal transverse steel ratio, leads to a decrease in the probability of ductile failure in the EBRIG strengthened RC specimens. Furthermore, comparing the energy absorption values of Group 1 and 2, exhibits that EBRIG technique is more capable to induce ductile failure in RC beams without stirrups. The energy absorption value of the specimen strengthened by the EBRIG method in Group 3, was 2300 J, showing a 31% enhancement, compared with its corresponding control beam.

It can be observed from Table 3 that more ductile failure modes occurred in the EBRIG strengthened beams made of normal strength concrete.

Table 3 further indicates that vertical grooves, via the EBRIG technique, increased the energy absorption by 85% and 97%, in beams with and without stirrups, respectively. However, the diagonal installation of CFRP strips in Group 4, improved the energy absorption value of specimens with and without stirrups by approximately 101% and 135%, respectively, implying the higher potential of inclined grooving to improve ductility compared to the vertical ones. Moreover, the results showed that the presence of stirrups limited the improvement of the ductility along with the maximum attained load.

3.3 Comparison of experimental results with design equations of the ACI code

According to the provisions in the available codes, the nominal shear resistance (V_n), can be defined as follows

$$V_n = V_c + V_s + V_f \tag{1}$$

Table 4 Maximum strain in the CFRP laminates and the predicted shear capacity of the beam

Group	Label	Maximum strain in CFRP (μs)	Predicted shear capacity by Eq. (1) (kN)	Experimental shear capacity (kN)	$\frac{V_{Experimental}}{V_{Predicted}}$
1	B1-EBRIG-V-30	7900	166	187	1.12
	B2-EBRIG-V-30	8600	194	225	1.15
	B3-Control-3	-	98	111	1.12
	B4-Control-30	-	113	129	1.14
	B5-EBR-V-30	3500	160	172	1.07
2	B6-EBRIG-V-30	9200	274	288	1.05
	B7-EBRIG-V-30	8900	245	269	1.09
	B8-Control-30	-	185	220	1.18
	B9-Control-30	-	173	181	1.05
3	B10-EBRIG-V-55	8600	298	336	1.12
	B11-Control-55	-	213	282	1.32
4	B12-EBRIG-D-30	9300	301	293	0.97
	B13-EBRIG-D-30	8800	213	251	1.17

Where V_c and V_s are the shear contributions of the concrete and stirrups and can be determined using the ACI 318 proposals (ACI committee 318 2014). The shear strength of the FRP system (V_f) can be computed by the provisions of the ACI 440.2R (ACI Committee 440 2008) in which accurate estimation of the effective strain is important in the bonded laminates. The maximum strain was measured using the DEMEC strain gauge (Table 4) in the present research of the beams failed by CFRP rupture. It is worthy to note that the strain value in the CFRP laminate is not the absolute ultimate value due to reading the magnitude of a gauge before the failure moment.

For the EBR strengthened specimens, the effective strain can be also estimated using the existing equations in the ACI 440.2R in which evaluation of the active bond length for the CFRP laminate is important (ACI Committee 440 2008). The Young's modulus and the thickness of the composite laminates (resin-rich fiber) were 42000 MPa and 0.6 mm, respectively, as reported by the manufacturer.

In Table 4, shear resistance computed by Eq. (1) was compared with the experimental data and agrees well with them. For all strengthened specimens (except for the specimen B12), Eq. (1) underestimates the total shear capacity of the tests. This can be attributed to the strain value in the CFRP laminate measured before CFRP rupturing. In addition, it is seen from $\frac{V_{Experimental}}{V_{Predicted}}$ ratio in Table 4 that addition of stirrups to the strengthened beams in Group 2, predicted the total shear capacity more accurately. According to Table 4, for the strengthened beams reinforced with stirrups, the maximum strain in CFRP laminate was more than the strengthened beams without stirrup. Based on the recorded strains, inclined EBRIG system contributed more in sustaining stresses than vertical one due to the orientation of CFRP strips that are perpendicular to the cracks. Note that the discrepancies related to the slippage of the loading steel plates or the sliding of the mounted strain gauge may result in lower value of the ultimate shear capacity or higher evaluation of the CFRP strip, respectively; this can be the reason for ratio of the shear capacity (less than one) in Table 4 for B12 specimen. For the EBRIG strengthened beams, the average value of the measured strain in the laminates was larger than 8800 μs and the CFRP laminates reached higher tensile capacity values.

4. Conclusions

The experiments carried out in the present work were aimed at investigating the potential of the recent EBRIG shear strengthening system in improving load carrying capacity and ductility as well as studying the shear performance of beam under static loading conditions. Based on the experimental observations and analytical investigations, the following conclusions can be derived:

- The EBRIG approach increases the contact area between embedded laminates and internal surfaces of the grooves (vertical or inclined) and improves interfacial bond between CFRP strips and concrete. Thus, it increases the maximum load and mid-span deflection and prevents a premature de-bonding of composite strips.
- The shear contribution of the EBRIG method in RC beams without stirrups increases with the rise in the ratio of longitudinal steel reinforcements; a 42% increase was recorded in the ultimate load as the longitudinal steel reinforcement ratio increased from 0.011 to 0.017.
- Increasing the ratio of stirrups in the EBRIG strengthened (via 90° grooves) beams, the ultimate load and mid-span deflection decreased by around 18% and 12%, respectively, relative to un-strengthened beams. The EBRIG strengthened beams failed due to rupture of CFRP strips compared to the EBR strengthened beams which experienced interfacial de-bonding of the composite laminates before shear failure.
- The EBRIG method is more effective in shear strengthening members made from normal strength concrete. The increase in the shear capacity of EBRIG strengthened beam of normal strength concrete and of the beams made of high strength concrete was 48% and 19%, respectively, suggesting the superiority of normal strength concrete.

• When vertical grooves were cut out through the EBRIG strengthening system, the energy absorption rate increased by 85% and 97% in RC beams with and without stirrups, respectively. In the case of utilizing diagonal grooves, the increase rates were 101% and 135%, respectively. These results corroborate the fact that, in comparison to vertical grooving, inclined grooving via EBRIG method is more capable of increasing the energy absorption rate in RC beams without stirrups.

• Experimental results indicated that the strain values in the CFRP laminates of the beams strengthened through the EBRIG method resulted in higher values in terms of the design strain limit (4000 μs) determined by the ACI 440.2R-08 code and may predict conservative values for the shear capacity of EBRIG strengthened beams.

Acknowledgments

The authors would like to thank Eng. Morovvati in MAT BETON PAYA for providing the ready-mix concrete.

Funding

This work received no financial support from any funding institute.

References

Abdel-Karim, A.A. (2014), "Shear strengthening of reinforced concrete beams with rectangular web openings by FRP composites", *Adv. Concrete Constr.*, **2**(4), 281-300.

Abdul, A.A., Ali, S.N. and Mohamad, N. (2017), "Shear strengthening and shear repair of 2-span continuous RC beams with CFRP strips", *J. Compos. Constr.*, **21**(3), 401- 412.

ACI 318R-4 (2014), Building Code Requirements for Structural Concrete and Commentary, American Concrete Institute; Farmington Hills, Michigan, USA.

ACI 440.2R-08 (2008), Guide for the Design and Construction of Externally Bonded FRP Systems for Strengthening Concrete MI, USA.

Al-Tersawy, S.H. (2013), "Effect of fiber parameters and concrete strength on shear behavior of strengthened RC beams", *Constr. Build. Mater.*, **44**, 15-24.

ASTM C 39/C 39M-04a (2005), Standard Test Method for Compressive Strength of Cylindrical Concrete Specimens, ASTM International, West Conshohocken, PA.

Belarbi, A. and Acun, B. (2013), "FRP systems in shear strengthening of reinforced concrete structures", *Procedia Eng.*, **57**, 2-8.

Chen, J.F. and Teng, J.G. (2003), "Shear capacity of FRP strengthened RC beam: FRP de-bonding", *Constr. Build. Mater.*, **17**(1), 27-41.

De Lorenzis, L. and Rizzo, A. (2009), "Behavior and capacity of RC beams strengthened in shear with NSM FRP Reinforcement", *Constr. Build. Mater.*, **23**, 1555-1567.

De Lorenzis, L. and Teng, J.G. (2007), "Near-surface mounted FRP reinforcement: an emerging technique for strengthening structures", *Compos. Part B Eng.*, **38**(2), 119-143.

Galal, K. and Mofidi, A. (2010), "Shear strengthening of RC T-beams using mechanically anchored un-bonded dry carbon fiber sheets", *J. Perform. Constr. Facil.*, **24**(1), 31-39.

Grande, E., Imbimb, M. and Rasulo, A. (2009), "Effect of transverse steel on the response of RC beams strengthened in shear by FRP-experimental study", *J. Compos. Constr.*, **13**(5), 405-414.

Gunes, O., Lau, D., Tuakta, C. and Buyukozturk, O. (2013), "Ductility of FRP- concrete systems: investigations at different length scales", *Constr. Build. Mater.*, **49**, 915-925.

Hosen, M.A., Jumaat, M.Z., Saiful Islam, A.B.M., Kamruzzaman, M., Nazmul Huda, M.D. and Rahman Soeb, M. (2015), "Eliminating concrete cover separation of NSM strengthened beam by CFRP end anchorage", *Struct. Eng. Mech.*, **56**(6), 899-916.

Kuntal, V.S., Chellapandian, M. and Prakash, S.S. (2017), "Efficient near surface mounted CFRP shear strengthening of high strength pre-stressed concrete beams-An experimental study", *Compos. Struct.*, **180**, 16-28.

Mesbah, H.A. and Benzaid, R. (2017), "Damage-based stress-strain model of RC cylinders wrapped with CFRP composites", *Adv. Concrete Constr.*, **5**(5), 539-561.

Mofidi, A. and Chaallal, O. (2014), "Effect of steel stirrups on shear resistance gain due to externally bonded fiber sheets", *ACI Struct. J.*, **111**(2), 353-362.

Mofidi, A., Chaallal, O. and Cheng, L. (2016), "Investigation of near surface–mounted method for shear rehabilitation of reinforced concrete beams using fiber reinforced–polymer composites". *J. Compos. Constr.*, **20**(2), 201-214.

Mostofinejad, D. and Mahmoudabadi, E. (2010), "Grooving as an alternative of surface preparation to postpone de-bonding of FRP lamination in concrete beams", *J. Compos. Constr.*, **14**(6), 804-811.

Mostofinejad, D. and Moshiri, N. (2014), "Compressive strength of CFRP composites used for strengthening of RC columns: Comparative evaluation of EBR and grooving methods", *J. Compos. Constr.*, **19**, 04014079.

Mostofinejad, D. and Shameli, S.M. (2013), "Externally bonded reinforcement in grooves (EBRIG) technique to postpone de-bonding of FRP sheets in strengthened concrete beams", *Constr. Build. Mater.*, **38**, 751-758.

Mostofinejad, D. and Tabatabaei Kashani, A. (2013), "Experimental study on effect of EBR and EBROG methods on de-bonding of FRP sheets used for shear strengthening of RC beams", *Compos. Part B Eng.*, **45**, 1704-1713.

Mostofinejad, D. and Torabian, A. (2015), "Experimental study of circular RC columns strengthened with longitudinal CFRP composites under eccentric loading: Comparative evaluation of EBR and EBROG methods on effect of EBR and EBROG methods", *J. Compos. Constr.*, **20**(2), 04015055.

Mostofinejad, D., Esfahani, M.R. and Shomali, A. (2019), "Experimental and numerical study of the RC beams shear-strengthened with NSM technique", *J. Compos. Mater.*, 0021998319830777.

Mostofinejad, D., Hosseini, S.A. and Razavi, S.B. (2016), "Influence of different bonding and wrapping techniques on performance of beams strengthened in shear using CFRP reinforcement", *Constr. Build. Mater.*, **116**, 310-320.

Rita, S.Y., Wong, F. and Vecchio, J. (2003), "Towards modeling of reinforced concrete members with externally bonded fiber reinforced polymer composites", *ACI Struct. J.*, **100**(1), 47-55.

Saljoughian, A. and Mostofinejad, D. (2018), "Grooving methods in square RC columns strengthened with longitudinal CFRP under cyclic axial compression", *Eng. Struct.*, **174**, 724-735.

Satish Kumar, C.N., Krishna, P.V. and Kumar, D.R. (2017), "Effect of fiber and aggregate size on mode-I fracture parameters of high strength concrete", *Adv. Concrete Constr.*, **5**(6), 613-624.

Shomali, A., Mostofinejad, D. and Esfahani, M.R. (2019), "Shear strengthening of RC beams using EBRIG CFRP strips: A

comparative study", *Eur. J. Environ. Civil Eng.*, **5**(6), 625-638.
Sumathi, A. and Arun Vignesh, S. (2017), "Study on behavior of RCC beams with externally bonded FRP members in flexure", *Adv. Concrete Constr.*, **5**(6), 625-638.
Teng, J.G., Chen, J.F., Smith, S.T. and Lam, L. (2002), *FRP Strengthened RC Structures*, John Wiley & Sons, USA.
Zhou, C., Ren, D. and Cheng, X. 2017, "Shear-strengthening of RC continuous T-beams with spliced CFRP U-strips around bars against flange top", *Struct. Eng. Mech.*, **64**(1), 135-143.

CC